Acoustic tomography techniques for observing atmospheric turbulence

D. Keith Wilson,[1] Vladimir E. Ostashev,[2,3] and Sergey N. Vecherin[2,1]

[1]U.S. Army Engineer Research and Development Center, Hanover, NH
[2]Physics Department, New Mexico State University, Las Cruces, NM
[3]NOAA/Earth System Research Laboratory, Boulder, CO

Geophysical Turbulence Phenomena Theme of the Year Workshop 3
Observing the Turbulent Atmosphere:
Sampling Strategies, Technologies, and Applications

Boulder, CO, 28-30 May 2008

Outline

- Introduction and brief history
- Acoustic travel-time tomography
  - Principle
  - Typical experimental designs
  - Comparison to other remote sensing techniques
- Inverse methods
  - Stochastic inverse and a priori statistical models
  - Time-dependent stochastic inverse
- Example experimental results
- Conclusions

Outline

- **Introduction and brief history**
- Acoustic travel-time tomography
  - Principle
  - Typical experimental designs
  - Comparison to other remote sensing techniques
- Inverse methods
  - Stochastic inverse and a priori statistical models
  - Time-dependent stochastic inverse
- Example experimental results
- Conclusions

Introduction

- Tomography, or “imaging by sections,” is used in many fields such as medicine, seismology, oceanography, and materials testing. A probing waveform is transmitted through a medium; received waveforms are then used to reconstruct the medium.
- Here, we describe acoustic travel-time tomography of the atmospheric surface layer. Travel-time variations of acoustic waveforms are used to reconstruct the wind-velocity and temperature fields.
- Some possible applications are (1) four-dimensional imaging of coherent structures, (2) validation of large-eddy simulation closure models, and (3) improvement of passive localization of sound sources.
- The inverse method used for the reconstructions is of prime importance. We discuss how *a priori* assumptions affect the reconstructions, and how information at multiple time steps can be used to improve them.

Brief History of Acoustic Travel-Time Tomography

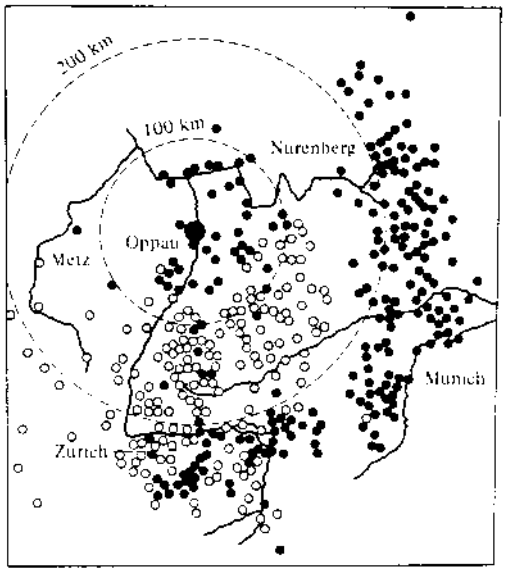

Zones of audibility of an explosion (from Cook, 1964)

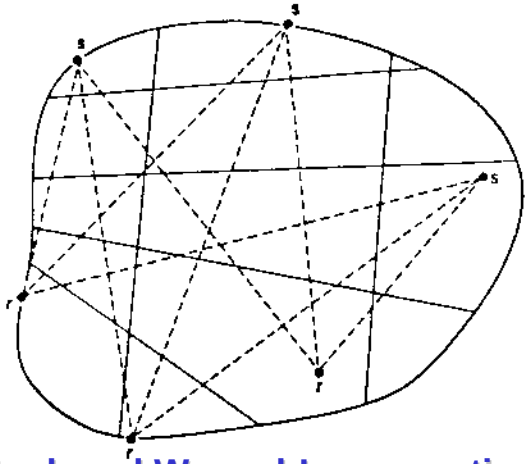

Munk and Wunsch's conception of horizontal slice ocean tomography (1978)

- Upper tropospheric and stratospheric wind and temperature profiles were deduced from explosions in early 1900's.
- Tomography for imaging ocean structure was first suggested by Munk and Wunsch (1978). This technique has since been widely and successfully applied to the ocean.
- Vertical slice tomography schemes proposed for the atmosphere by Greenfield et al (1974), Ostashev (1982), Chunchuzov et al (1990), and Klug (1989), among others.
- Application of horizontal-slice tomography to near-ground atmosphere was first suggested by Spiesberger (1990). First experimental implementation was reported by Wilson and Thomson (1994). Ziemann, Arnold, and Raabe, et al have since performed numerous indoor and outdoor experiments.

Tomographically reconstructed wind and temperature fields (Wilson and Thomson 1994)

The experiment involved 3 sources and 5 receivers (15 propagation paths). Shown are horizontal slices with dimensions 200 m by 200 m, at a height of 6 m. The images are spaced by about 12 sec.

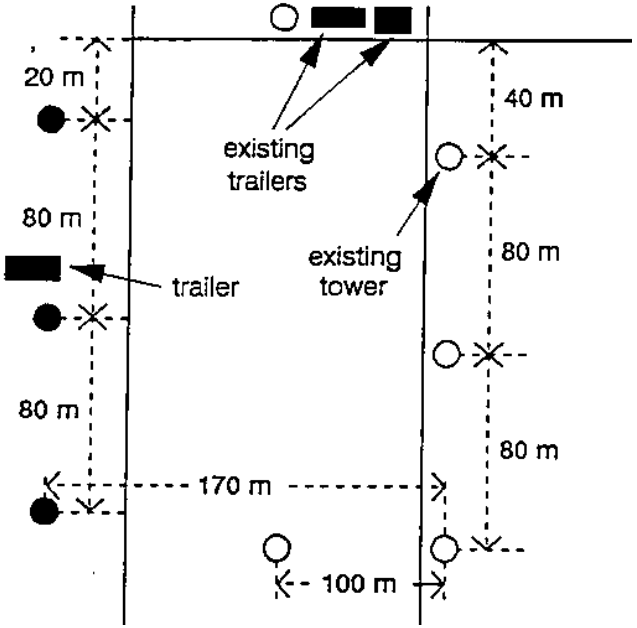

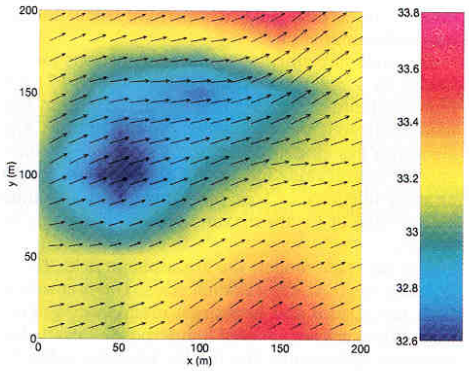

FIG. 18. Horizontal-slice reconstruction at the 6-m height from session 8, data cycle 79. The arrows represent wind speed and direction, with maximum length corresponding to 6 m s^{-1}. The color scale represents virtual temperature in degrees Celsius.

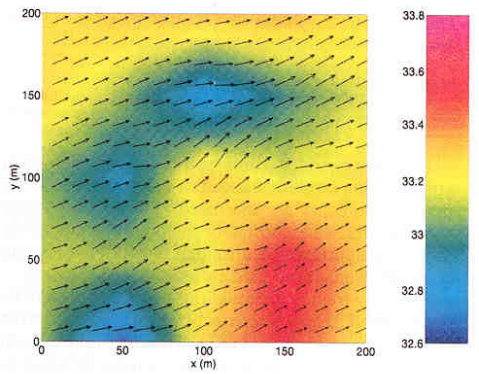

FIG. 19. Reconstruction, data cycle 82.

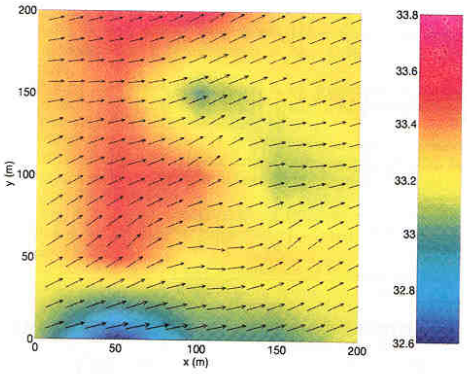

FIG. 20. Reconstruction, data cycle 85.

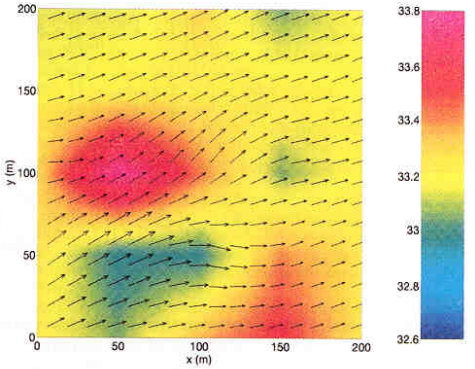

FIG. 21. Reconstruction, data cycle 88.

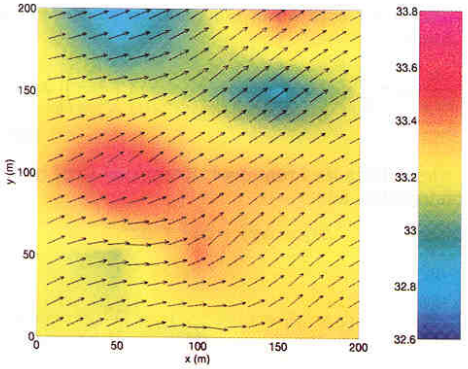

FIG. 22. Reconstruction, data cycle 92.

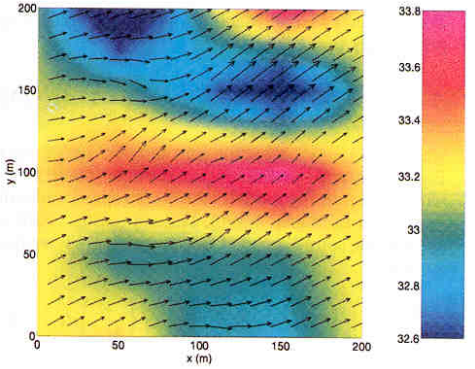

FIG. 23. Reconstruction, data cycle 94.

Outline

- Introduction and brief history
- Acoustic travel-time tomography
  - Principle
  - Experimental design considerations
  - Comparison to other remote sensing techniques
- Inverse methods
  - Stochastic inverse and a priori statistical models
  - Time-dependent stochastic inverse
- Example experimental results
- Conclusions

Dependence of Sound Speed on Temperature, Humidity, and Wind

$$c = \sqrt{\left(\frac{\partial P}{\partial \rho}\right)_{adiabatic}} = \sqrt{\frac{\gamma P}{\rho}} = \sqrt{\gamma R T}$$

fluid | **ideal gas**

For humid air,

$$c = 20.05\sqrt{T}\left(1 + 0.258q\right) = 20.05\sqrt{T_v}\left(1 - 0.046q\right)$$

absolute temperature | ***water vapor mixing ratio*** | ***virtual temperature***

With wind,

$$\frac{d\mathbf{x}}{dt} = c\mathbf{n} + \mathbf{u}, \quad \frac{d\mathbf{n}}{dt} = -\nabla_\perp c - \sum_{i=1}^{3} n_i \nabla_\perp u_i$$

If the propagation direction is nearly constant, i.e., $\mathbf{s} = (\hat{e}_x, 0, 0)$, the ray equations are approximately

$$\frac{d\mathbf{x}}{dt} = c_{eff}\mathbf{n}, \quad \frac{d\mathbf{n}}{dt} = -\nabla_\perp c_{eff}$$

where the "effective" sound speed is

$$c_{eff} = c + u_x$$

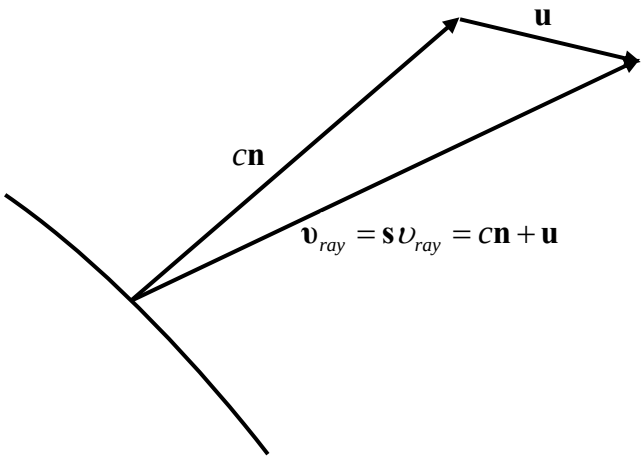

Index-of-Refraction Fluctuations: Sound Compared to Light

Keeping only the temperature contribution, the acoustic index of refraction is

$$n_{sound} = \frac{c_0}{c} \approx 1 - \frac{T'}{2T_0}$$

For light (with temperature in K and pressure in mbar),

$$\frac{c_{vacuum}}{c} = 1 + 77.6 \times 10^{-6} \frac{P}{T}$$

This leads to

$$n_{light} = 1 + 77.6 \times 10^{-6} \left(\frac{P}{T} - \frac{P_0}{T_0} \right) \approx 1 - 77.6 \times 10^{-6} \frac{P_0 T'}{T_0^2}$$

Hence the ratio of the fluctuations in index of refraction is

$$\frac{n'_{sound}}{n'_{light}} = \frac{-T'/2T_0}{-77.6 \times 10^{-6} \, P_0 T' / T_0^2} = 6.44 \times 10^3 \frac{T_0}{P_0}$$

With T_0 = 300 K and P_0 = 1000 mbar,

$$\frac{n'_{sound}}{n'_{light}} \approx 2000$$

Acoustic “Thermometry” and “Flow Velocimetry”

Reciprocal transmissions allow the sound speed and along-path wind speed to be uniquely determined.

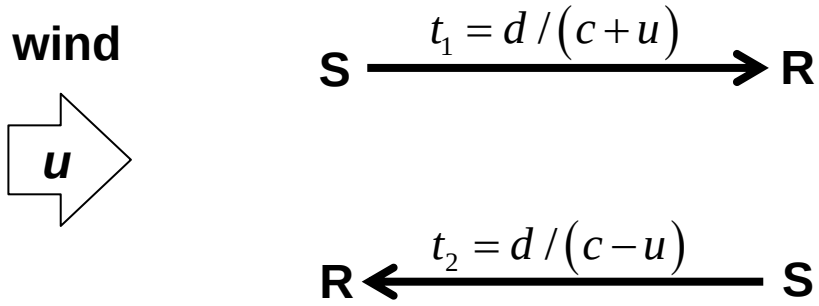

$$c = \frac{d}{2}\left(\frac{1}{t_1} + \frac{1}{t_2}\right) \qquad u = \frac{d}{2}\left(\frac{1}{t_1} - \frac{1}{t_2}\right)$$

The ultrasonic anemometer/thermometer is an example of a device that uses the travel time of acoustic pulses to infer sound speed (temperature) and wind velocity.

Acoustic "Thermometry" or "Flow Velocimetry" vs. Acoustic Travel-Time Tomography

Tomography also uses travel-time data to infer sound speed and wind velocity. *Additionally*, an attempt is made to reconstruct the spatial structure of the atmospheric fields, rather than simply determining them at a single "point."

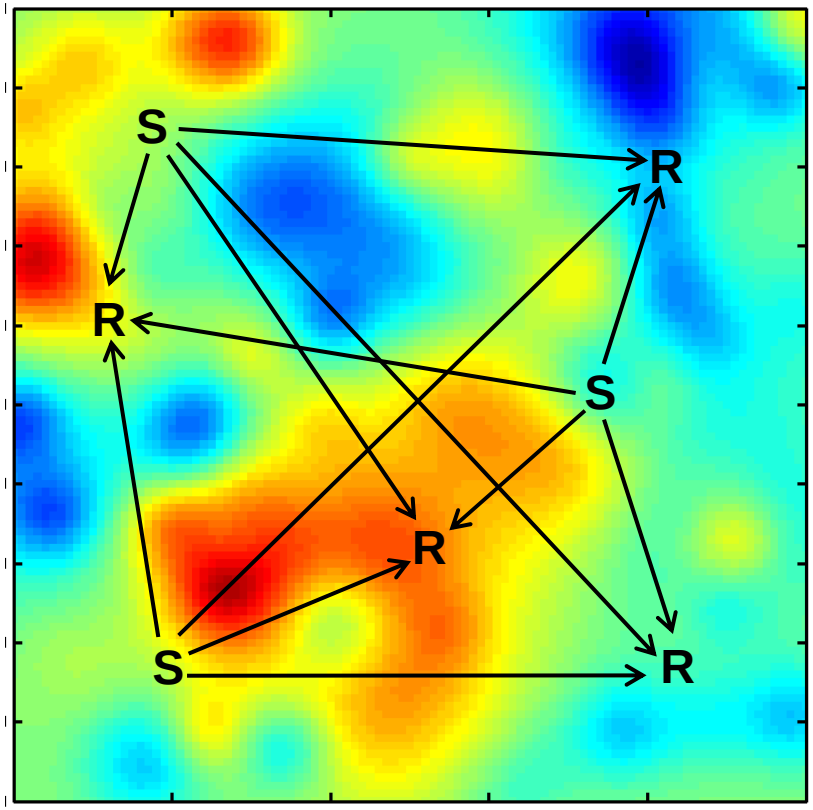

- **Note that the number of data points is N_s x N_r, where N_s is the number of sources and N_r the number of receivers.**
- **When a flow is present, the travel time depends on the direction of propagation.**
- **Travel-time data, rather than attenuation data (like in medical ultrasonics), is used.**

Experimental Design Considerations

The design of an acoustic tomography experiment must address several (sometimes competing) design considerations. In particular:

- **Travel time estimates must be very accurate (better than 0.1 ms). Bandwidth of the signal and SNR control the accuracy of the estimates.**
- **Frequency must not be too high, or absorption will rapidly attenuate signal.**
- **Frequency should not be too low, or ray approximations will break down.**
- **The inverse problem is easier if the ray paths can be approximated as straight lines, which favors short paths and weak vertical gradients.**

Comparison to Other Atmospheric Remote Sensing Systems

- Acoustic tomography provides 2D or 3D fields. (Main alternatives are arrays of in situ sensors, lidar, volume-imaging radar, PIV?)
- It simultaneously yields both the temperature and wind fields (in situ sensors and RASS also).
- Generally optimal for very low altitudes (unlike radar, sodar, or RASS).
- Data are *path averages,* unlike point sensors but similar to other remote sensing techniques.
- The cost of instrumentation is low, but generally requires a distributed array (set up at multiple towers).
- The range is short (few hundred meters or less) for current designs. (Infrasonic tomography could be practiced a much longer ranges.)
- The signal processing (inverse method) is complicated and still a topic for research.
- There is a possibility for noise disturbance (potentially worse than sodar or RASS, because beam is not vertical).

Outline

- Introduction and brief history
- Acoustic travel-time tomography
  - Principle
  - Typical experimental designs
  - Comparison to other remote sensing techniques
- **Inverse methods**
  - **Stochastic inverse and a priori statistical assumptions**
  - **Time-dependent stochastic inverse**
- Example experimental results
- Conclusions

Tomographic Data Inversions: Issues

- *What inverse methods are suitable for reconstructions of atmospheric turbulence fields?*
- *What* a priori *knowledge is required for satisfactory reconstructions?*
- *What are the benefits of path-integrated observations (tomography) as opposed to point observations?*
- *How should the transmission paths be arranged? Are reciprocal transmissions required to simultaneously determine sound speed and wind effectively?*

Inverse Problem Formulation

- **The N_m unknown atmospheric parameters (*models*) are grouped into a column vector $\mathbf{m}$.**

  The models consist of the atmospheric fields (wind and temperature) at a number of points in space where direct observations are unavailable.

- **The N_d atmospheric observations (*data*) are grouped into a column vector $\mathbf{d}$.**

  The data are either point measurements of the atmospheric fields (conventional observations) or travel times of acoustic pulses along the propagation paths (tomography).

- **The *inverse problem* is to construct an operator $\mathbf{G}_x^{-1}$ that provides a model estimate $\hat{\mathbf{m}}$ from the data. For a linearized inverse,**

$$\hat{\mathbf{m}} = \mathbf{G}_x^{-1}\mathbf{d}$$

Optimal Stochastic Inverse

It can be shown that the optimal inverse operator, in the sense of minimizing the expected mean-square errors $\left\langle e_j^2 \right\rangle = \left\langle \left(\hat{m}_j - m_j \right)^2 \right\rangle$ **, is**

$$\mathbf{G}_s^{-1} = \mathbf{R}_{md}\mathbf{R}_{dd}^{-1}$$

where

$\mathbf{R}_{md} = \left\langle \mathbf{m}\mathbf{d}^{\mathrm{T}} \right\rangle$ **is the model-data cross-correlation matrix**

$\mathbf{R}_{dd} = \left\langle \mathbf{d}\mathbf{d}^{\mathrm{T}} \right\rangle$ **is the data autocorrelation matrix**

The operator $\mathbf{G}_s^{-1}$ **is called the *stochastic inverse* in the geophysics literature.**

- **Both** $\mathbf{R}_{dd}$ **and** $\mathbf{R}_{md}$ **can be determined from the correlation functions for the atmospheric fields. The principle difficulty in setting up the optimal stochastic inverse is that the correlation functions are not known in advance.**
- **Therefore, the optimal (*true*) stochastic inverse is unattainable in most real-world problems.**
- **In practice, *we use the propagation physics to model the relationship between the data and models, and assume a correlation function for the models*.**

Other Inverse Approaches and Implications for the Reconstructed Field

- **Interpolation methods.** ***These approaches usually assume a smooth variation, obeying a prescribed spline function, of the field between the observation points.***
- **Approaches based on grid-cell partitioning (generalized inverse, Monte Carlo, …)** ***These approaches usually assume perfect correlation between two points within the same grid cell, and no correlation if they are in different grid cells.***
- **Spatial harmonic series.** ***Usually, a discrete spectrum is used with a finite series of spatial wavenumber components. This introduces a fundamental period and smoothness into the reconstructed fields.***

None of these approaches are free of assumptions regarding the spatial structure of the reconstructed field!

Since the problem of reconstructing a spatial continuous medium from finite measurements is inherently an underdetermined one, it would seem impossible to devise inverse methods that do not involve assumptions about the spatial structure of the model space.

Example Sensor Array

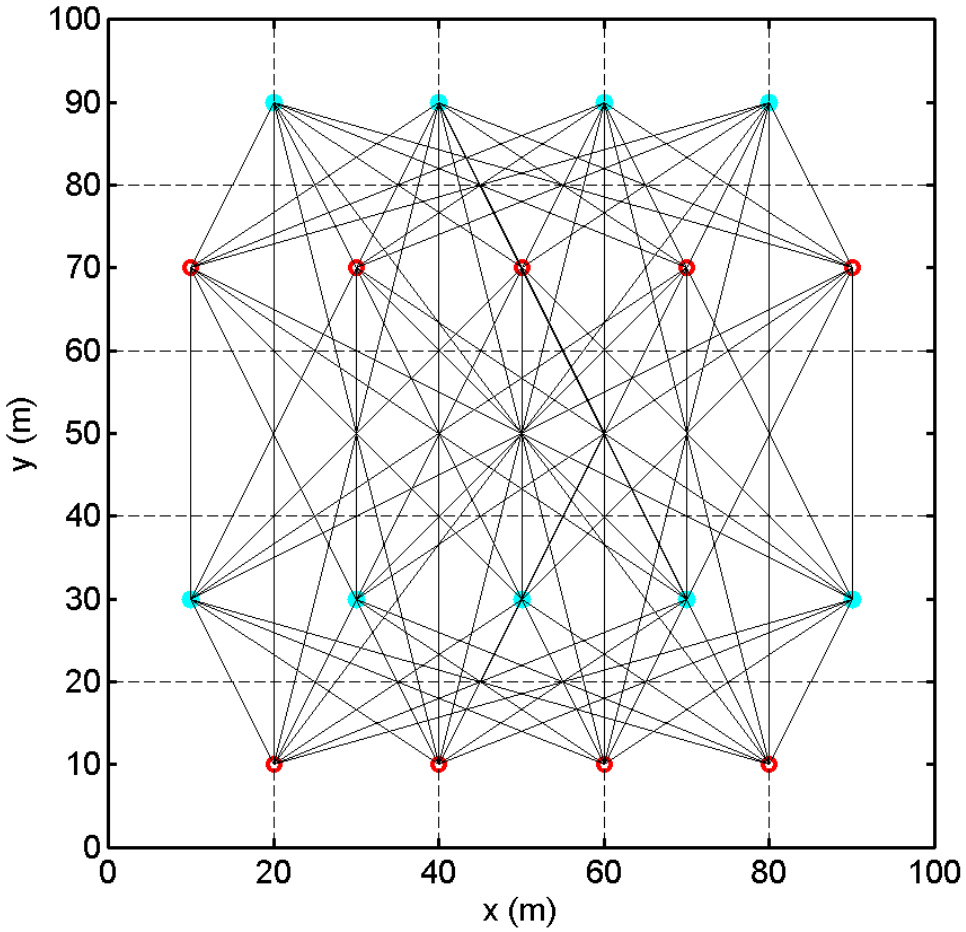

Cyan circles are positions of acoustic sources.

Red circles are positions of acoustic receivers.

Lines are the transmission paths.

For examples with point in situ sensors, identical sensors are located at *both* the cyan and red circles.

A horizontal plane configuration is studied here for simplicity. Many other schemes are possible, such as a vertical planar array in combination with Taylor's hypothesis to achieve 3D reconstructions.

Stochastic Inverse Examples (Point Sensors)

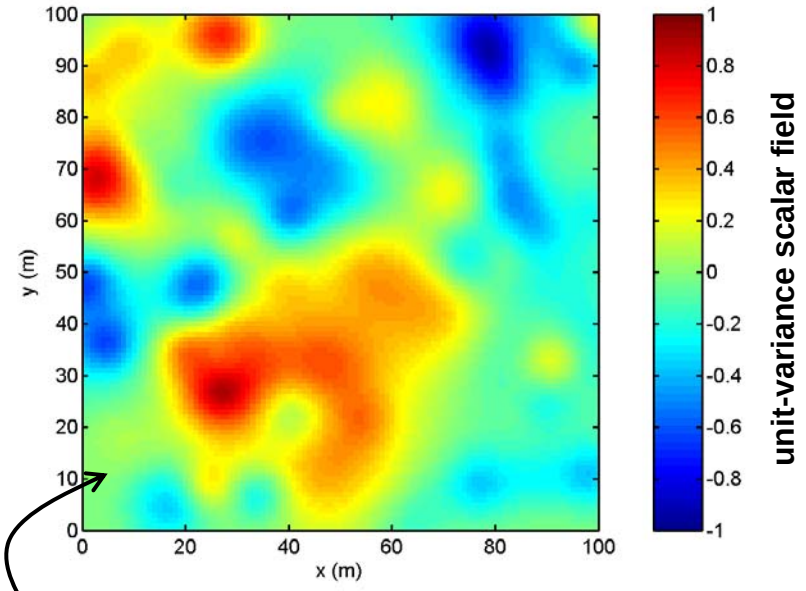

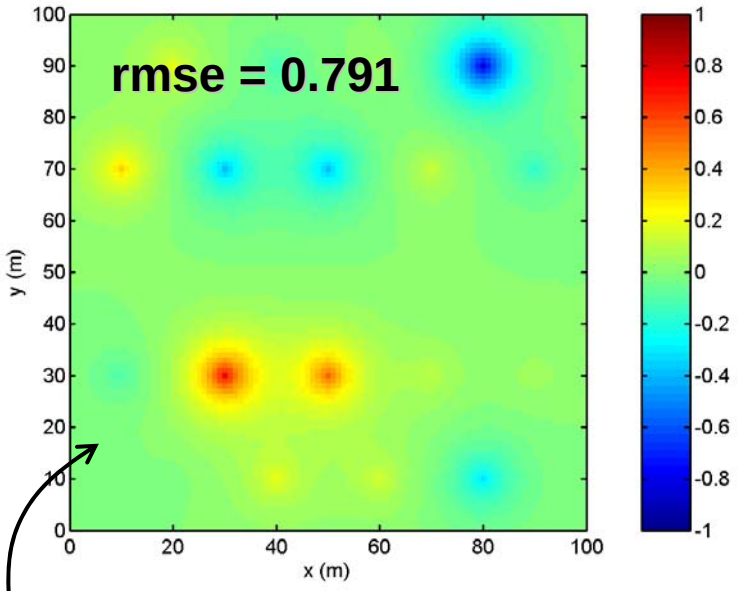

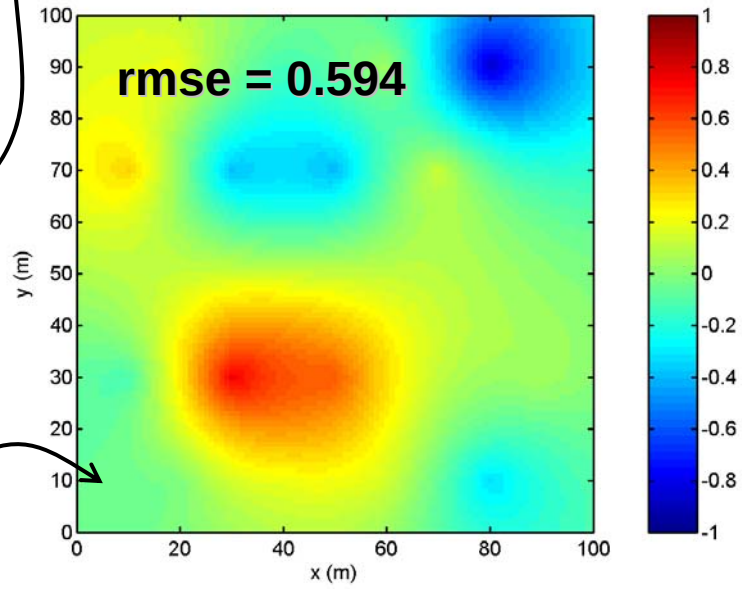

(1) Original synthetic scalar field. Spectrum is similar to a von Karman model for low Reynolds number turbulence (inner scale 5 m, outer scale 25 m).

(2) Stochastic inverse reconstruction for point sensor experiment. Presumed correlation is Gaussian with length scale 5 m.

(3) Stochastic inverse reconstruction for point sensor experiment. Presumed correlation is Gaussian with length scale 25 m.

Stochastic Inverse Examples (Tomography)

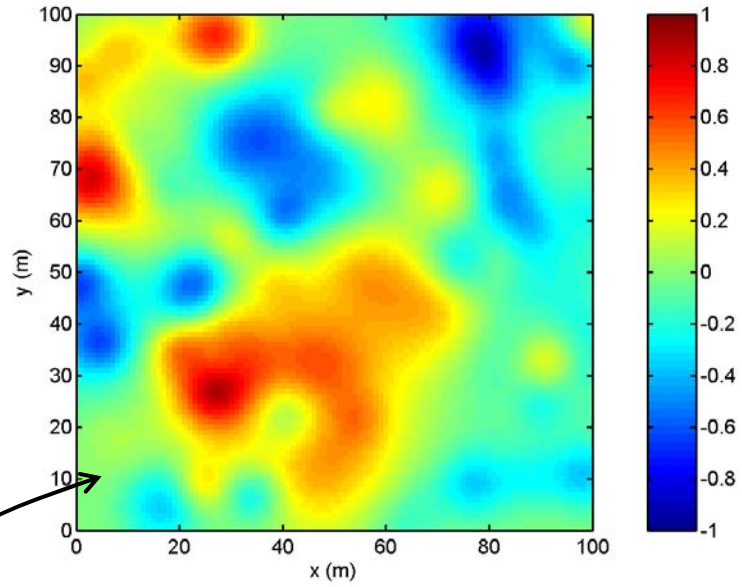

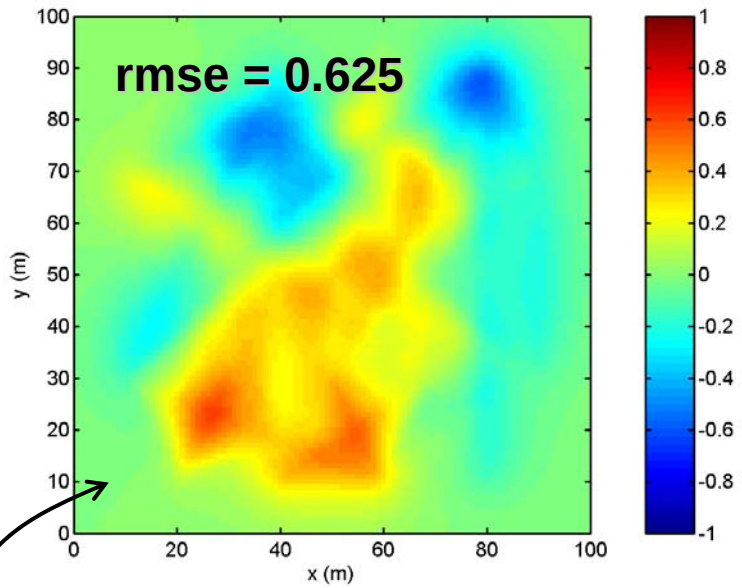

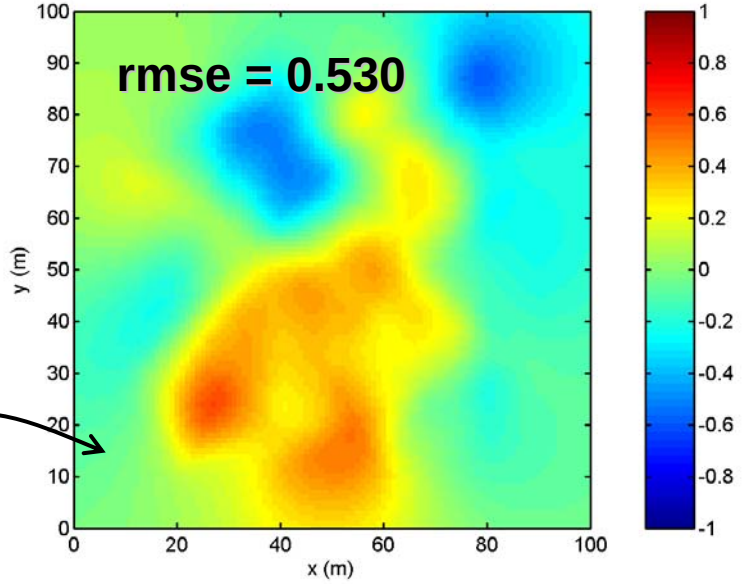

(1) Original synthetic scalar field. Spectrum is similar to a von Karman model for low Reynolds number turbulence (inner scale 5 m, outer scale 25 m).

(2) Stochastic inverse reconstruction for tomography experiment. Presumed correlation is exponential with length scale 5 m.

(3) Stochastic inverse reconstruction for tomography experiment. Presumed correlation is exponential with length scale 25 m.

Generalized Inverse Examples (Tomography)

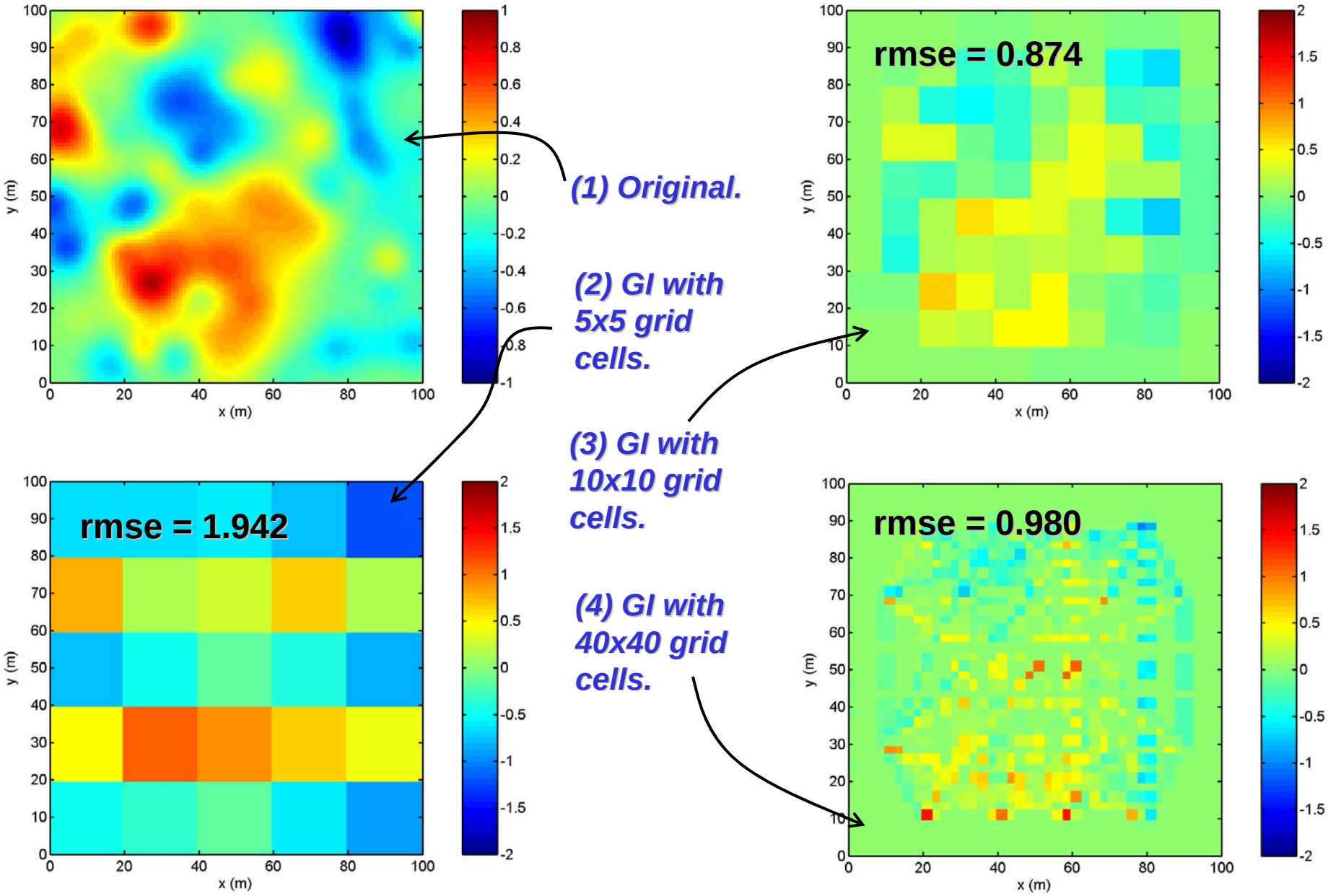

Example Correlation Functions

Von Karman (realistic for turbulence!):

$$f(r) = \frac{2\sigma^2}{\Gamma(1/3)}\left(\frac{r}{2\xi_K}\right)^{1/3} K_{1/3}\left(\frac{r}{\xi_K}\right)$$

Gaussian (*not* realistic for turbulence!):

$$f(r) = \sigma^2 \exp\left(-\frac{r^2}{\xi_G^2}\right)$$

Exponential (realistic at small separation):

$$f(r) = \sigma^2 \exp\left(-\frac{r}{\xi_e}\right)$$

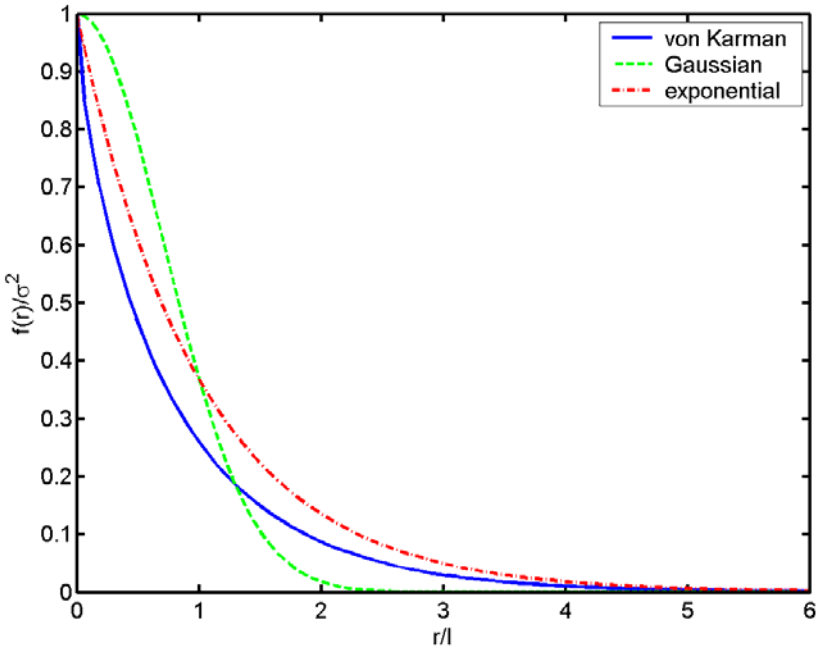

where σ^2 is the variance and the ξ's are length scales.

Effect of Correlation Function/Length Scale Mismatch

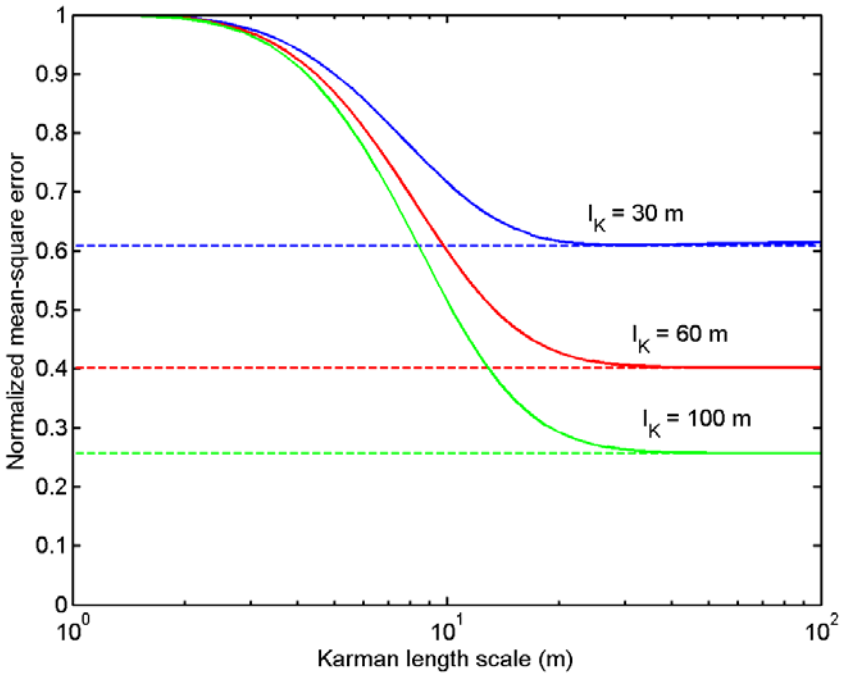

Mean-square error at the point (30m,40m) when the presumed and actual correlation functions are both vK, but the presumed length scale (the abscissa) does not match the actual (curves for three values shown).

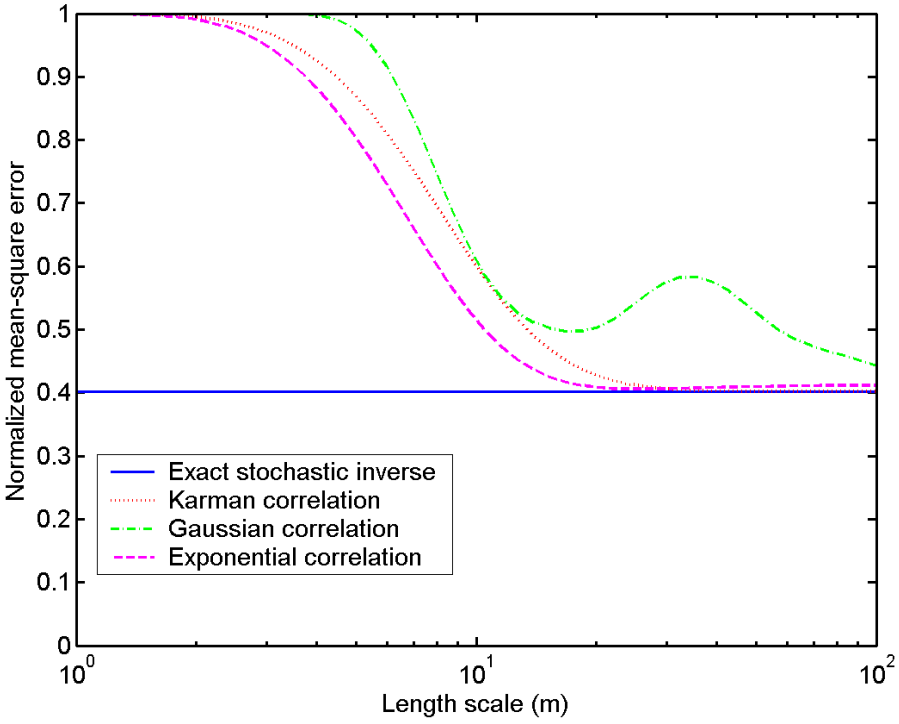

Mean-square error at the point (30m,40m) when the actual correlation function is vK and the length scale is 60 m. The presumed length scale and correlation function both vary from the actual.

Validation of SGS Schemes for LES

- **Wyngaard and Peltier (1996): "…the gap between our ability to produce calculations of the structure of turbulent flows and to test these calculations against data … seems wider than ever in micrometeorology."**
- **The spatial averaging inherent to tomography potentially makes it attractive for testing LES.**

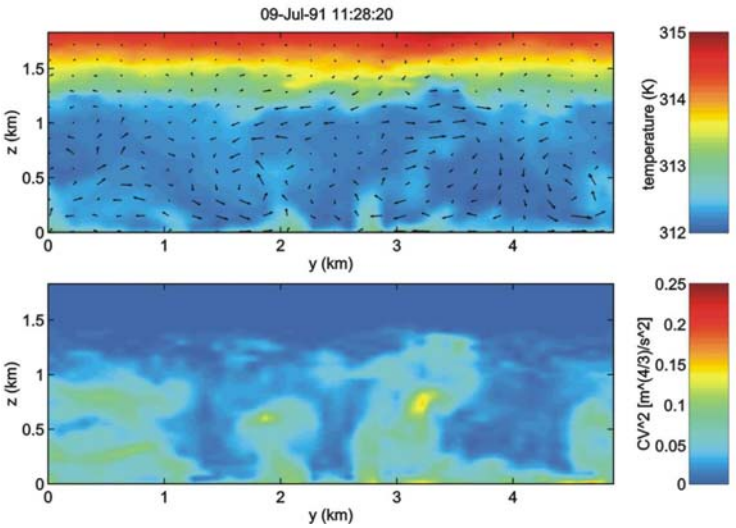

By definition, LES partitions the atmospheric fields into resolved-scale and subgrid-scale (SGS) components. The resolved component is explicitly simulated.

$$m(\mathbf{x},t) = m_r(\mathbf{x},t) + m_s(\mathbf{x},t)$$

total field — resolved field — SGS field

$$m_r(\mathbf{x},t) = \int F(\mathbf{x}-\mathbf{x}')m(\mathbf{x},t)d\mathbf{x}'$$

filtering function

The fidelity of LES depends on how well the *impact of the SGS structure* on the *resolved structure* is parameterized. Hence direct validation of LES must mimic the filtering function.

Comparison of Filtering with Tomography and Point Sensors

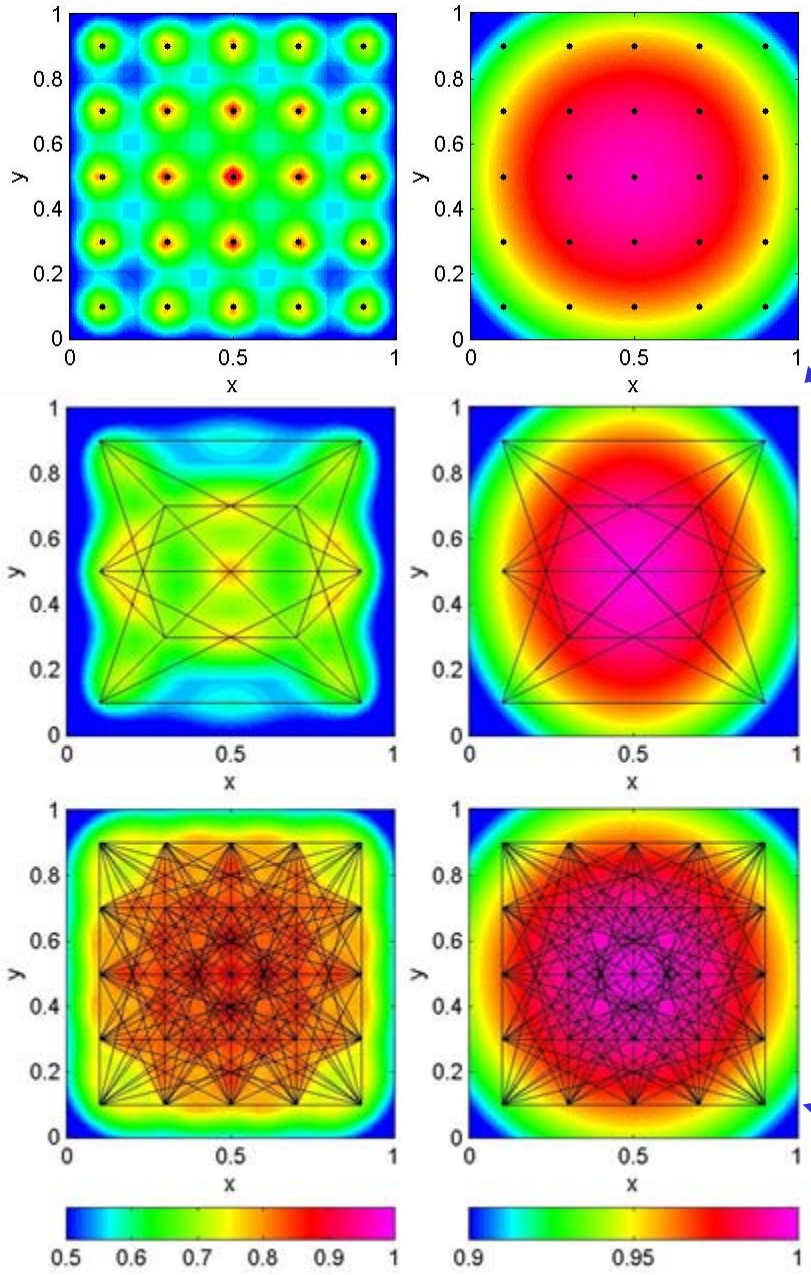

Left **column: correlation coefficient between estimated and actual *subgrid-scale* structure**

Right **column: correlation coefficient between estimated and actual *resolved-scale* structure**

A von Karman spectrum with length scale 1 was used for all calculations.

The filter function was:

$$F(x,y)=\begin{cases}1, & |x|\le 0.5 \text{ and } |y|\le 0.5\\ 0, & \text{otherwise}\end{cases}$$

25 point sensors

tomography with 5 srcs, 5 rcvrs (25 paths)

tomography with 13 srcs, 12 rcvrs (156 paths)

Time-Dependent Stochastic Inversion (TDSI)

Main idea: Determine current state using information at *prior, current*, and *future* time levels in inverse.

Implementation: The travel times are measured repeatedly. The temperature and wind velocity are assumed to be random functions in space and time with known spatial-temporal correlation functions (locally frozen turbulence).

TDSI increases the amount of data without increasing the number of sources and receivers!

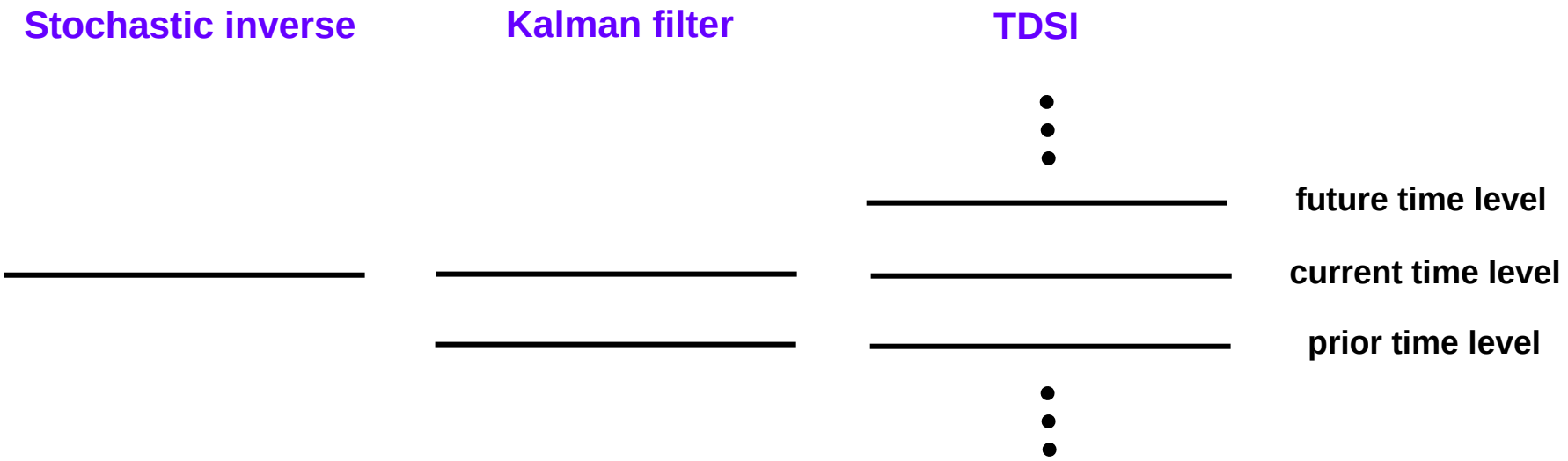

TDSI: Locally Frozen Turbulence

Frozen turbulence: $T(\mathbf{x}, t_2) = T(\mathbf{x} - \mathbf{v}_0 (t_2 - t_1), t_1)$.

Correlation function:

$$B_T(\mathbf{x}, t_1) = B_T(\mathbf{x} - \mathbf{v}_0 t_1) = \sigma_T^2 \exp\left(-|\mathbf{x} - \mathbf{v}_0 t_1|^2 / L^2\right).$$

Locally frozen turbulence:

$$T(\mathbf{x}, t_2) = T\left(\mathbf{x} - \mathbf{v}(\mathbf{x}, t_1)(t_2 - t_1), t_1\right), \qquad \mathbf{v}(\mathbf{x}, t) = \mathbf{v}_0 + \mathbf{v}(\mathbf{x}, t)$$

Correlation function:

$$B_T(\mathbf{x}, t) = \frac{\sigma_T^2}{\left(1 + 2\sigma_v^2 t^2 / L^2\right)^{3/2}} \exp\left[-\frac{|\mathbf{x} - \mathbf{v}_0 t|^2}{L^2 \left(1 + 2\sigma_v^2 t^2 / L^2\right)}\right].$$

Reconstruction of fluctuations in wind component (v_x)

(a)

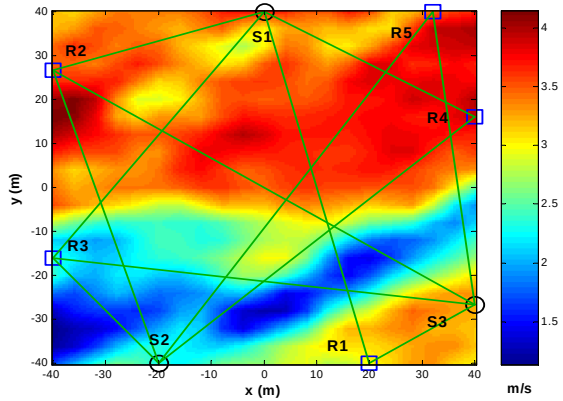

Large-eddy simulation, with tomographic array overlaid

Transducer locations were determined by an optimization procedure and correspond to upper-level of the BAO array.

(b)

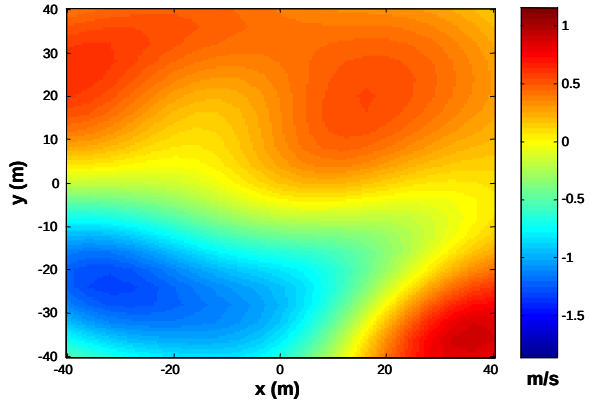

Stochastic inverse (SI)
Normalized RMSE is 0.37.

(c)

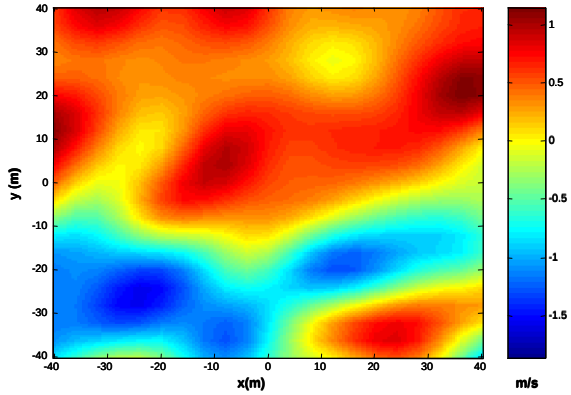

TDSI with 7 time steps
Normalized RMSE is 0.22.

The data grid consists of 400 pts and 3 fields. Nonetheless, TDSI provides an excellent reconstruction from just 15 travel times (at each time level).

3D Array for Acoustic Tomography (Similar to BAO Array Design)

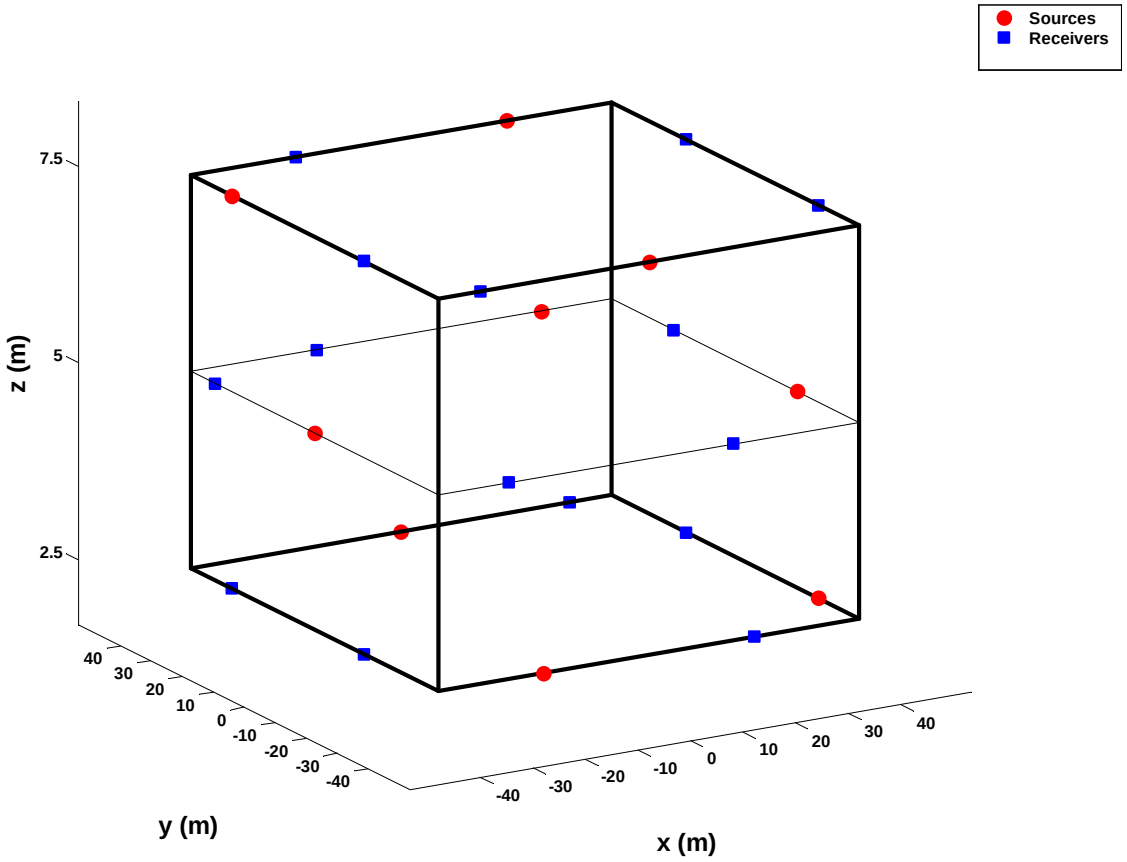

TDSI was generalized to 3D.

Wind velocity component, v

LES

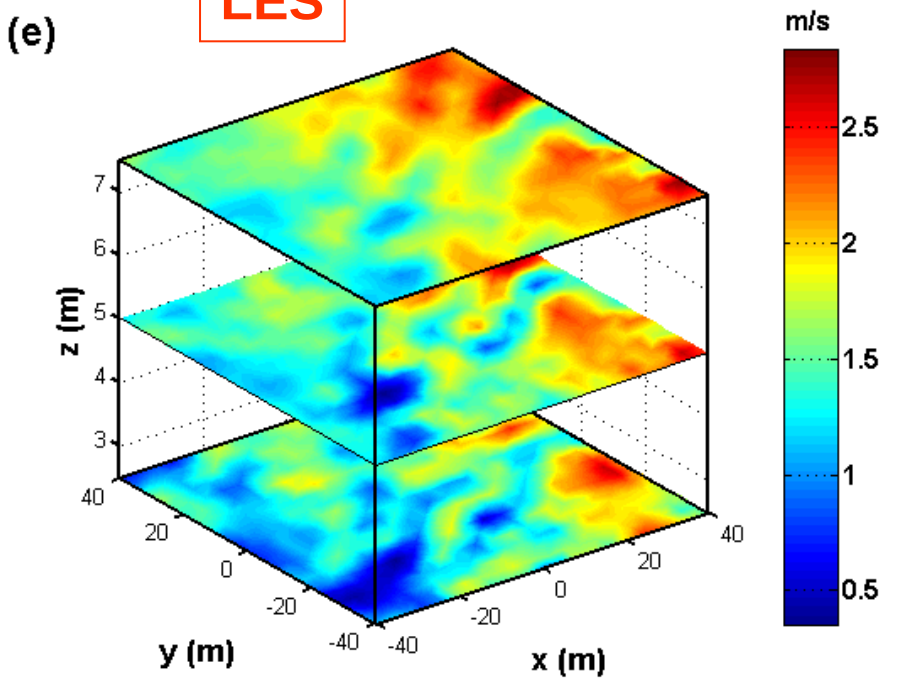

TDSI

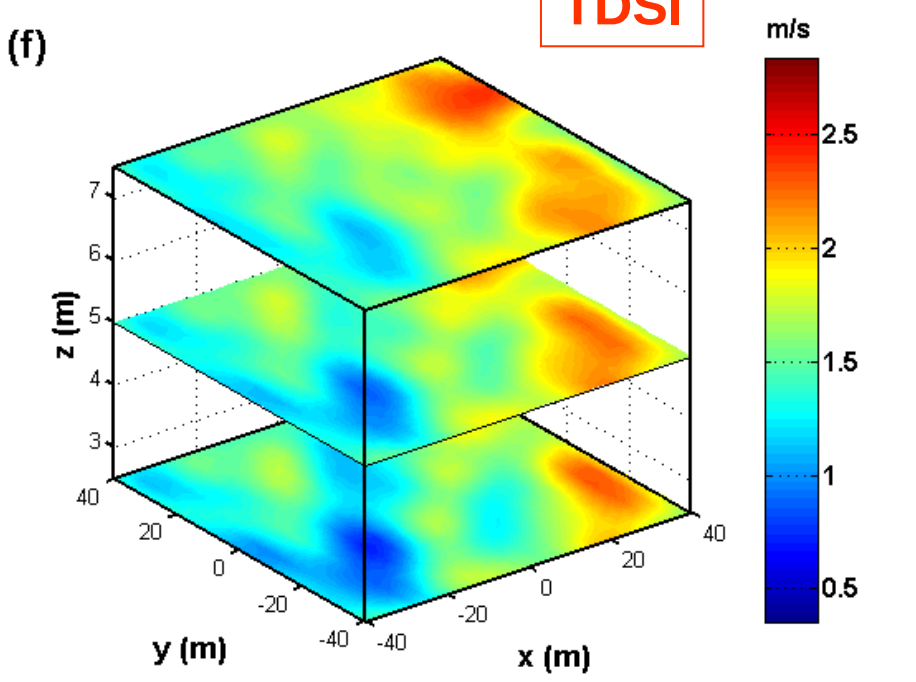

How to visualize 3D fields?

RMSE	T_{av} (¢)	$\tilde{u}$ (m/s)	$\tilde{v}$ (m/s)	$\tilde{w}$ (m/s)
Actual	0.10	0.34	0.26	0.19
Expected	0.13	0.31	0.24	1.1

Temperature reconstruction

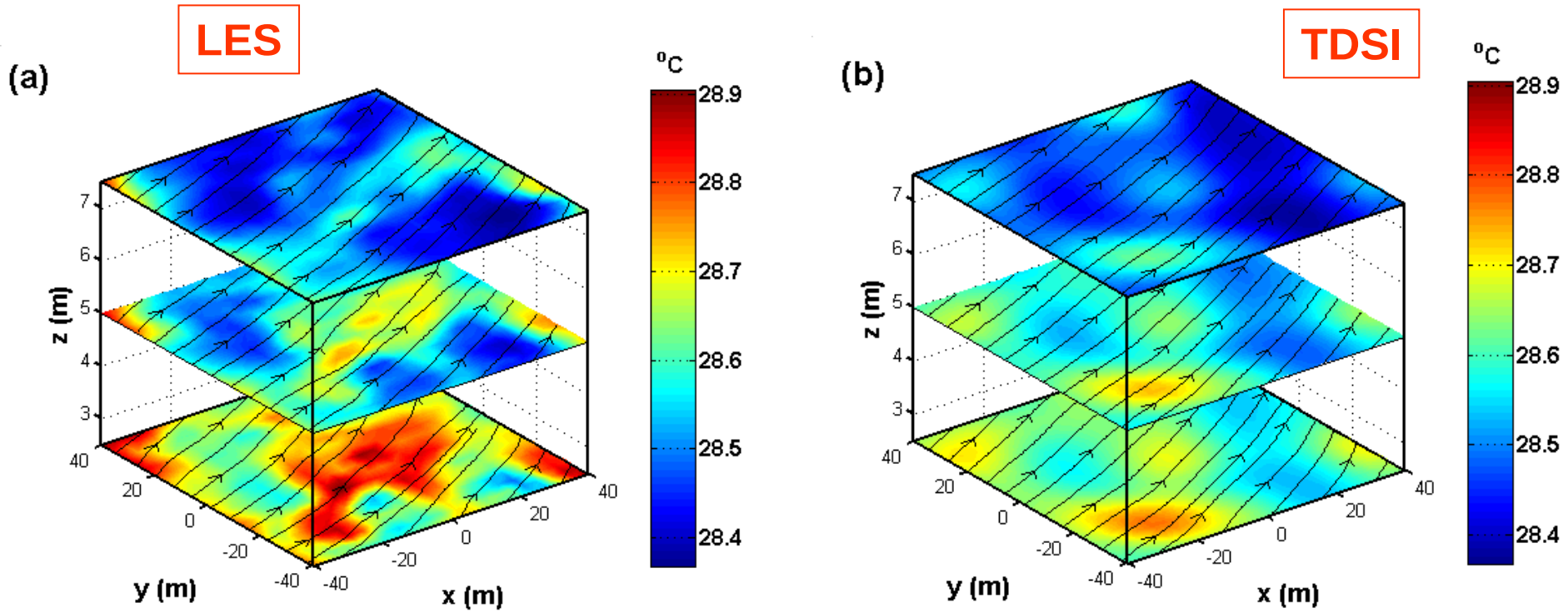

RMSE	T_{av} (¢)	$\tilde{u}$ (m/s)	$\tilde{v}$ (m/s)	$\tilde{w}$ (m/s)
Actual	0.10	0.34	0.26	0.19
Expected	0.13	0.31	0.24	1.1

Outline

- Introduction and brief history
- Acoustic travel-time tomography
  - Principle
  - Typical experimental designs
  - Comparison to other remote sensing techniques
- Inverse methods
  - Stochastic inverse and a priori statistical models
  - Time-dependent stochastic inverse
- **Example experimental results**
- Conclusions

Outdoor tomography experiment (STINHO)

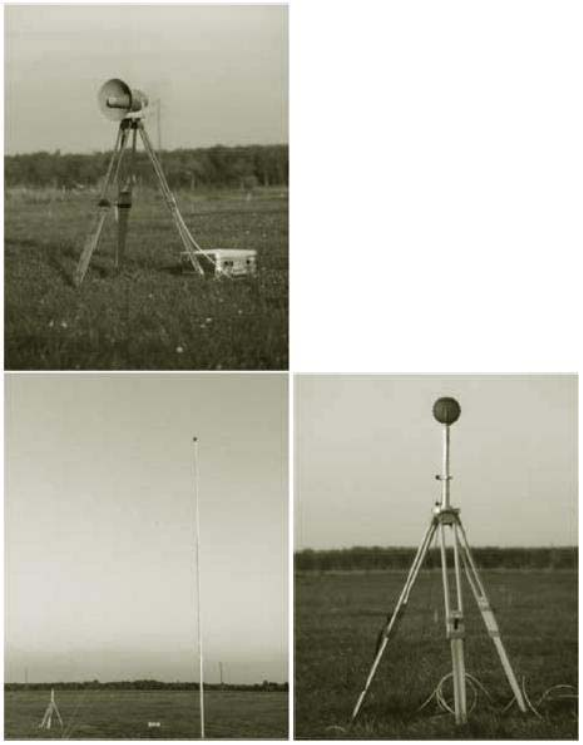

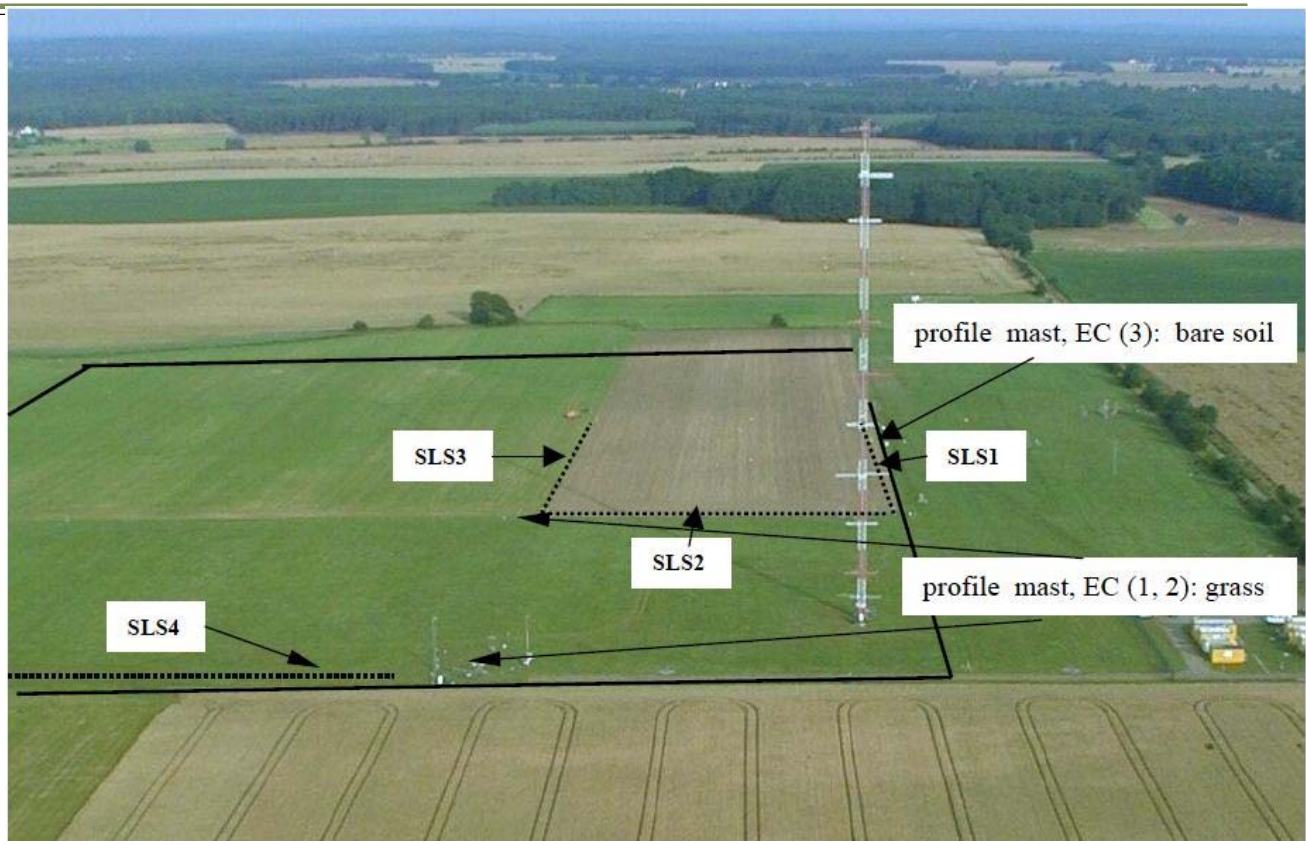

- STINHO: the effects of heterogeneous surface on the turbulent heat exchange and horizontal turbulent fluxes.
- Extensive meteorological equipment was deployed to measure parameters of the ABL.
- Experimental site: grass and bear soil.

Outdoor tomography experiment (STINHO)

Acoustic tomography experiment STINHO carried out by the University of Leipzig, Germany.

8 sources and 12 receivers located 2 m above the ground. Size of the array 300 x 440 m.

Travel times were measured every minute on 6 July 2002.

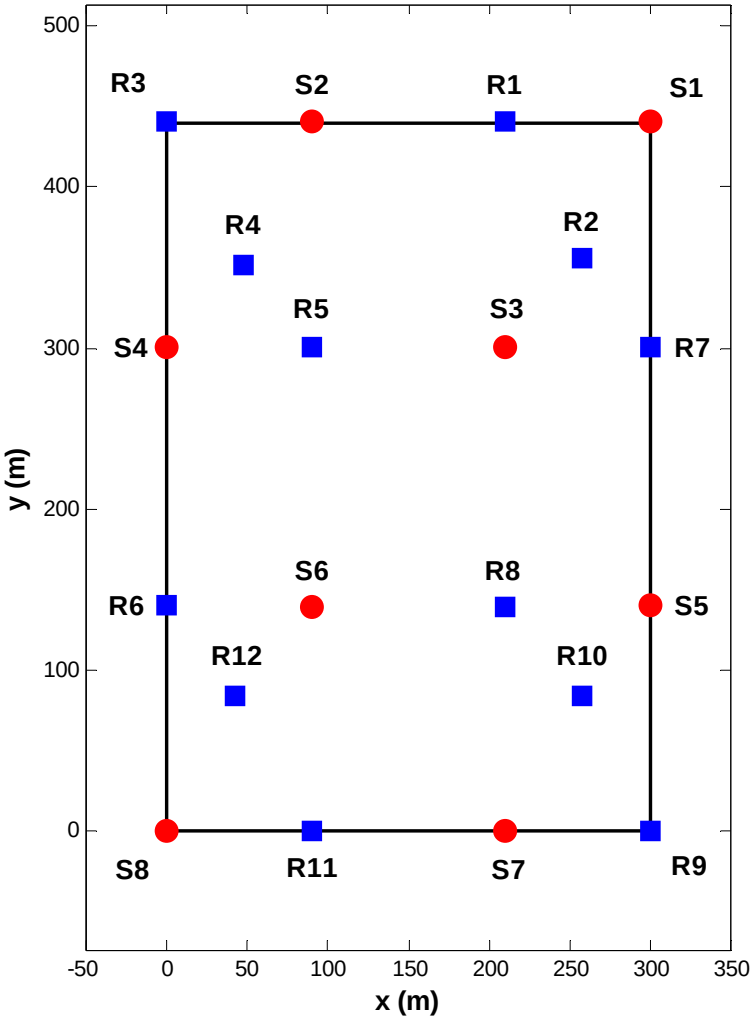

Reconstruction of mean fields

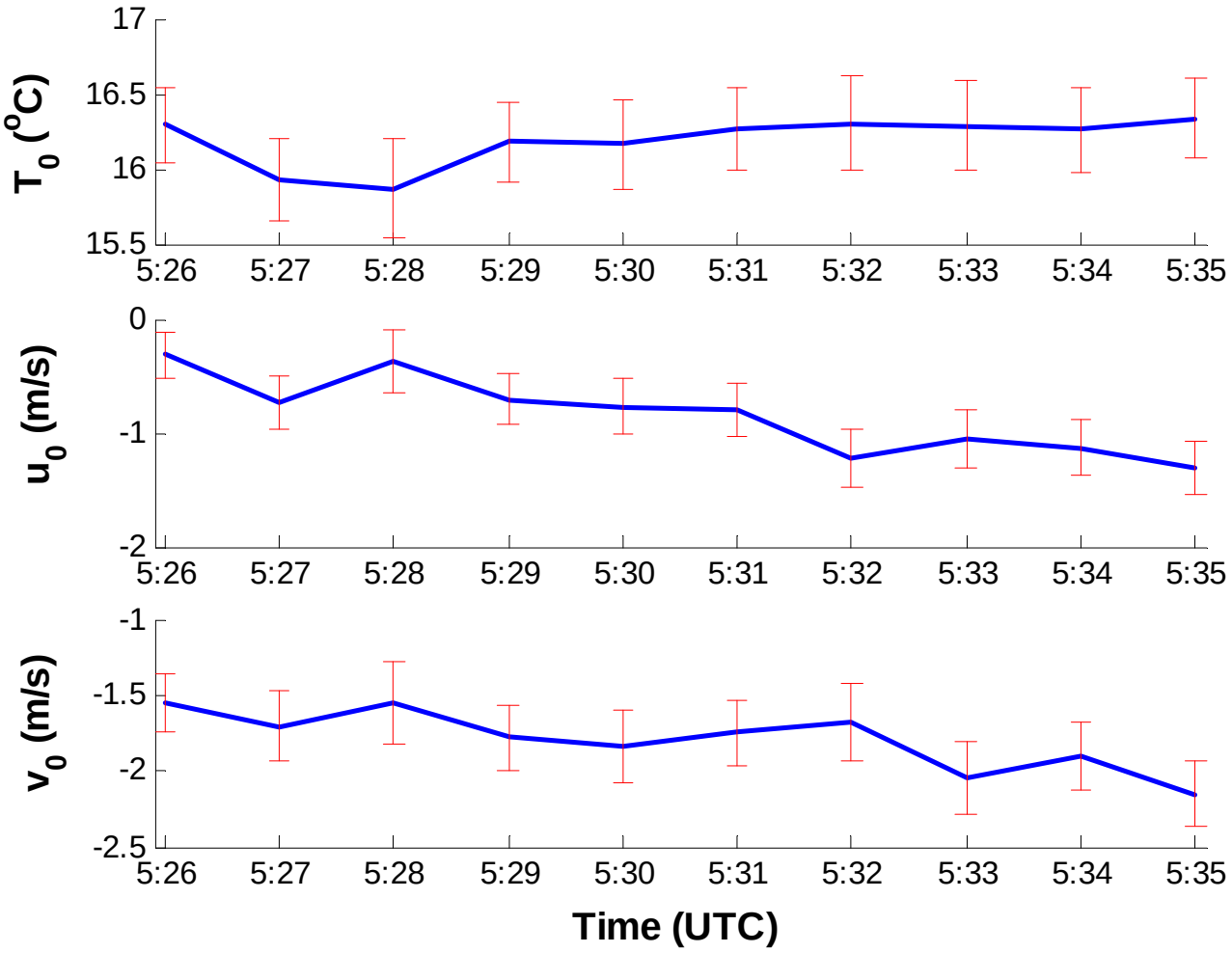

Reconstruction of fluctuations and total fields

US Army Corps of Engineers

ERDC

Reconstruction at 5:30 a.m. Three levels of travel times were used.
RMSE are 0.36 K, 0.35 m/s and 0.26 m/s.

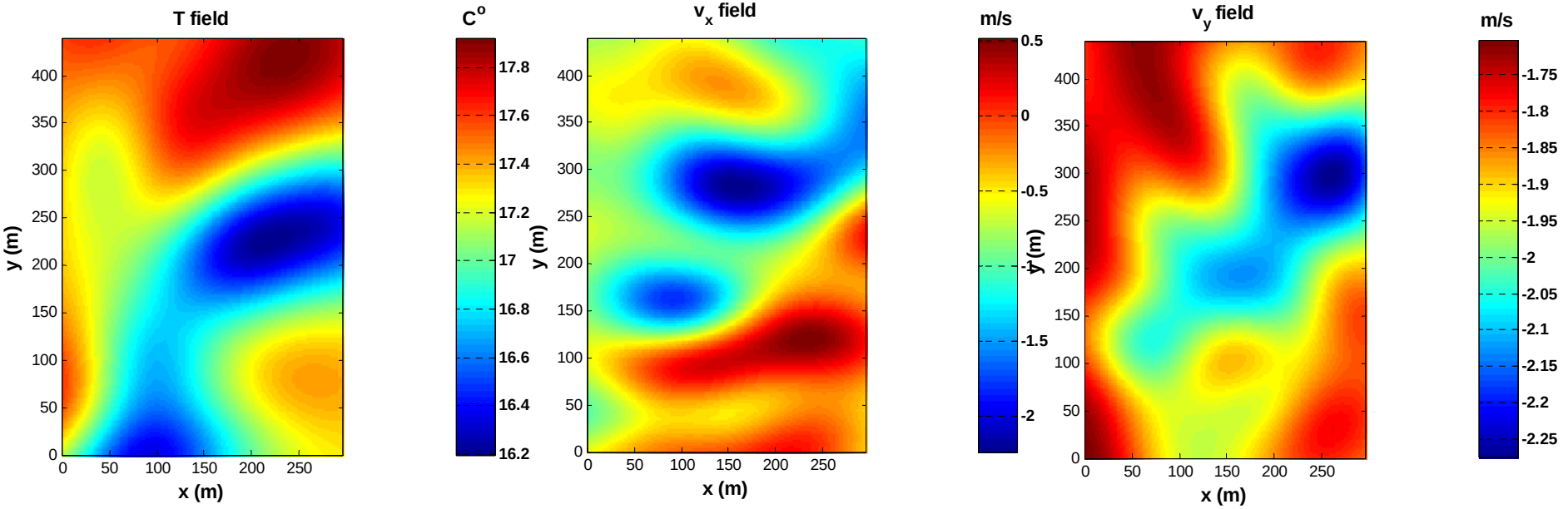

Landscape type	Coordinates (m)	Humitter T (¢)	TDSI T (¢)
Bare soil	x=28, y=138	16.24	16.14
Grassland	x=182, y=143	15.78	15.77

Expected errors of reconstruction

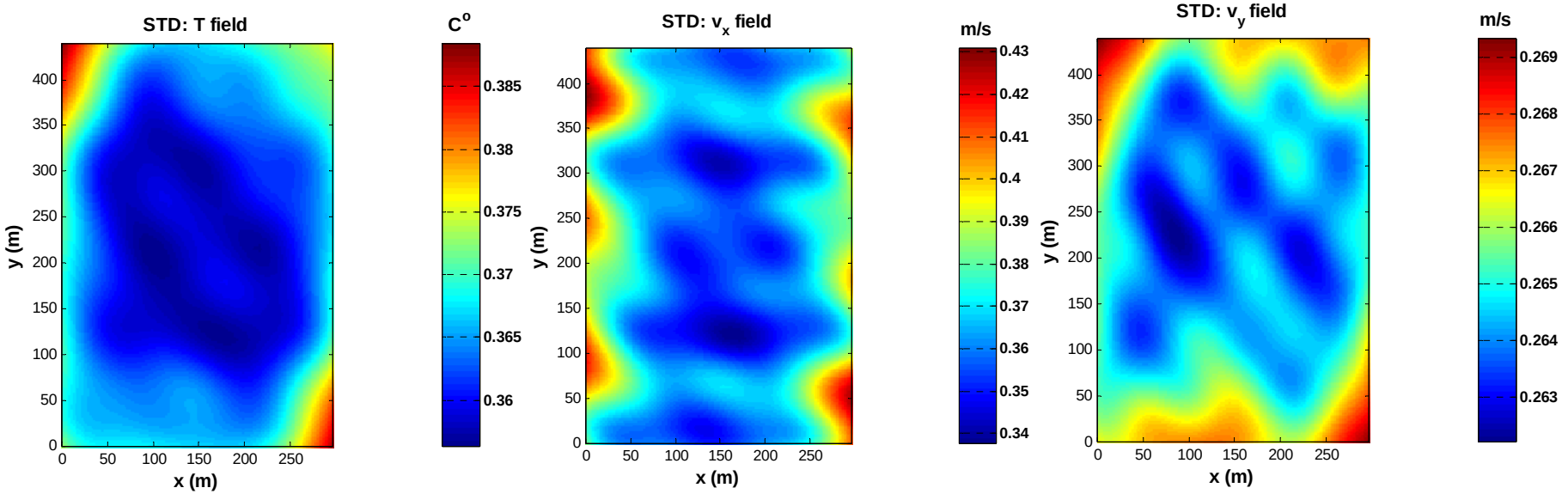

RMSE are 0.36 K, 0.35 m/s and 0.26 m/s.

Temperature field: 5:26 – 5:35 a.m.

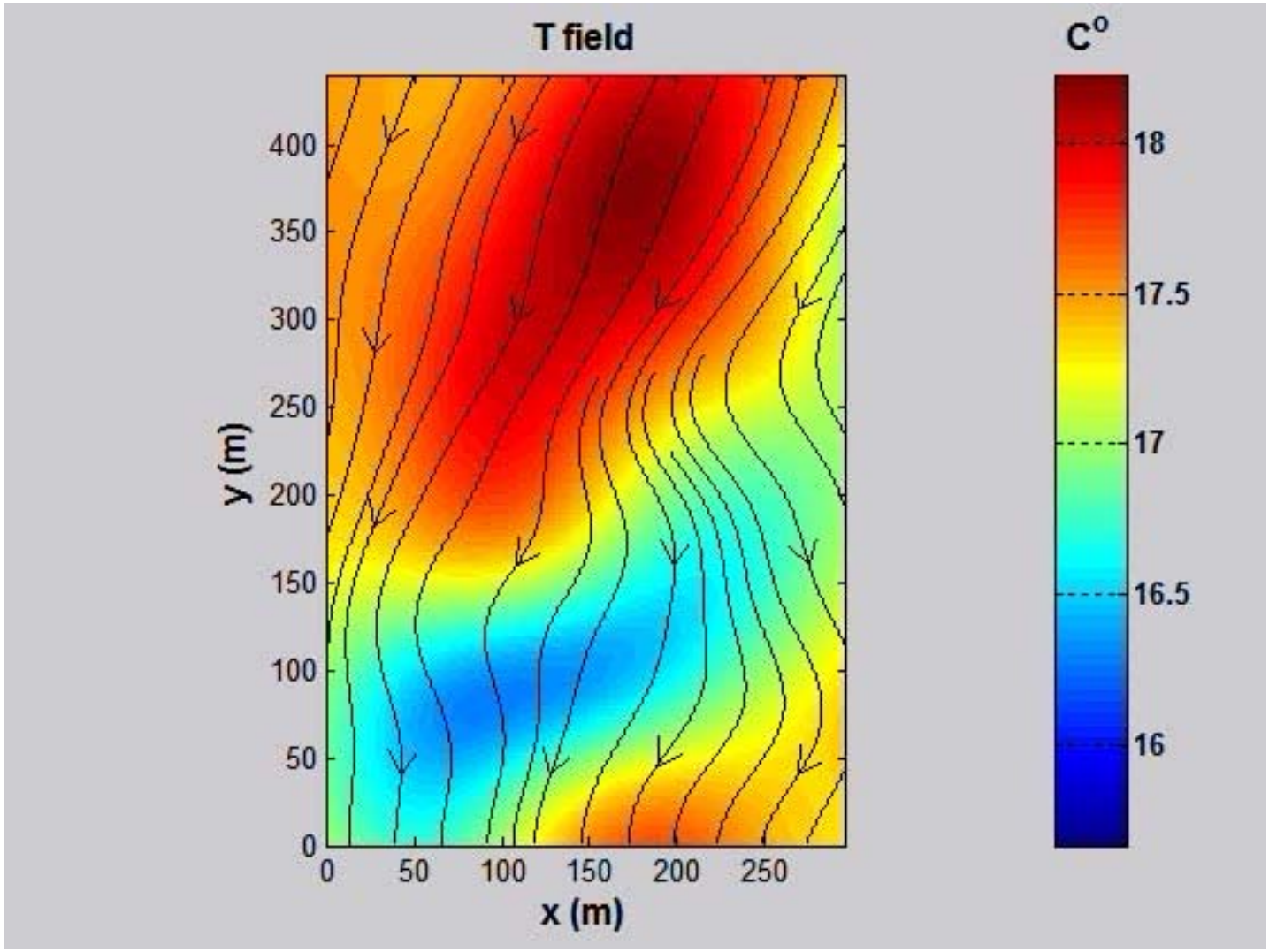

BAO Acoustic Tomography Array

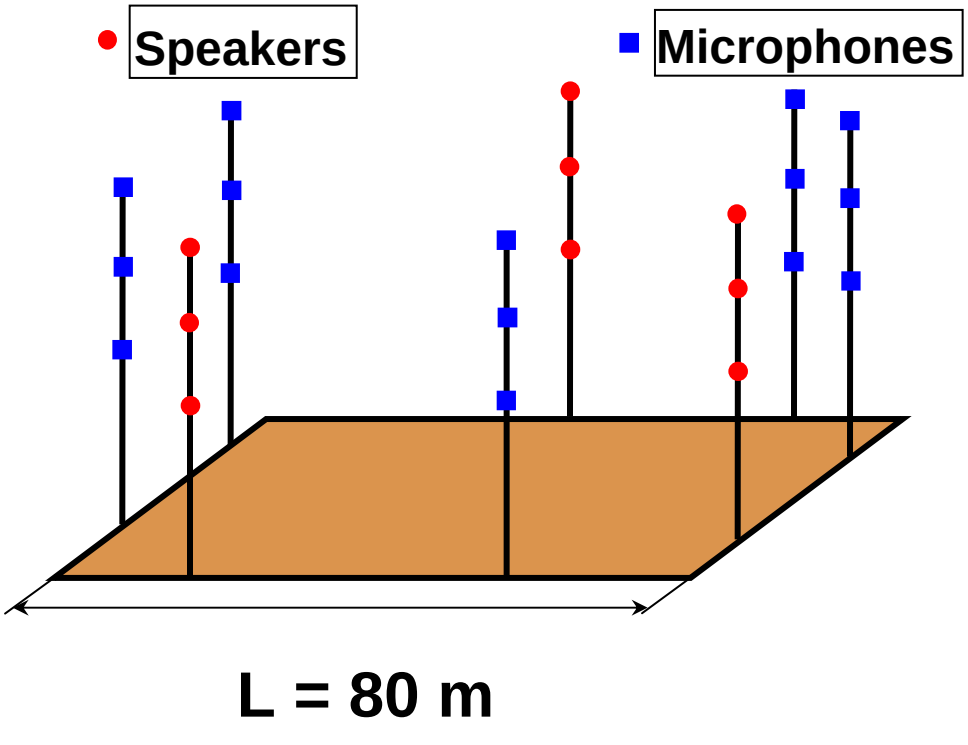

- NOAA/CIRES personnel involved in experimental implementation of ATA:
  A. Bedard, B. Bartram, C. Fairall, J. Jordan, J. Leach, R. Nishiyama, V. Ostashev, D. Wolfe.
- The bend-over towers are 30 feet high.
- The array became operational in March, 2008 (with transducers at the upper level only.)
- This is the only existing array for ATA in the U.S.
- Unlike previous array designs, it does not need to be dismantled.

BAO Acoustic Tomography Array

One tower is bent over. Building on left is the new Visitor Center.

Current Experimental Procedure for BAO Array

1. A sound signal is 10 periods of a pure tone of 1 kHz, in a Hanning window. (We might change this latter.)

2. To avoid overlapping of signals, speakers are activated in a sequence with 0.5 s delay, for 5-10 minutes continuously. (Latter, this will be increased for 1 h).

3. To ensure synchronization of speakers and microphones, they are connected to the central computer via cables (laid in trenches).

4. The emitted signals are cross-correlated with those recorded by microphones to get travel times of sound propagation.

5. After the travel times are measured, the TDSI algorithm is used for reconstruction of temperature and velocity fields.

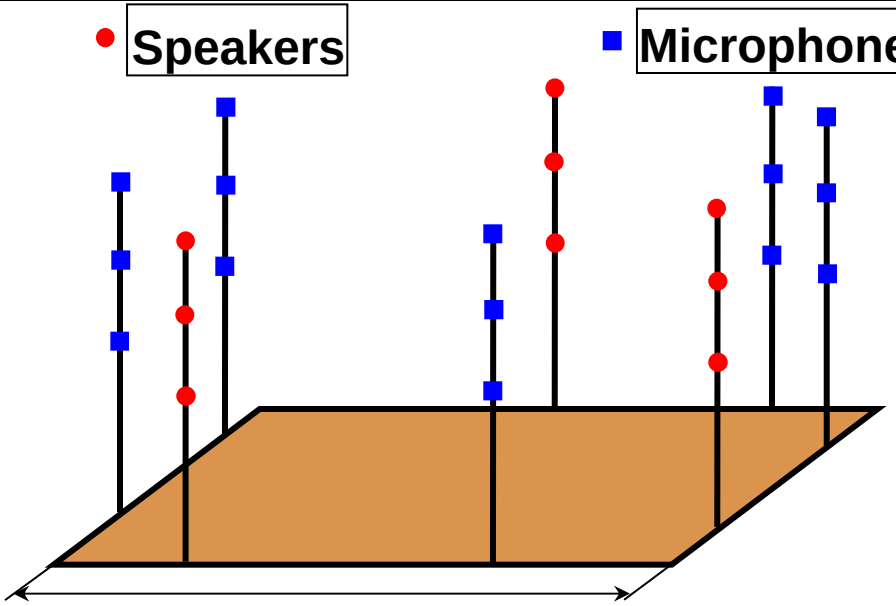

Examples of emitted and received signals on 3/37/2008

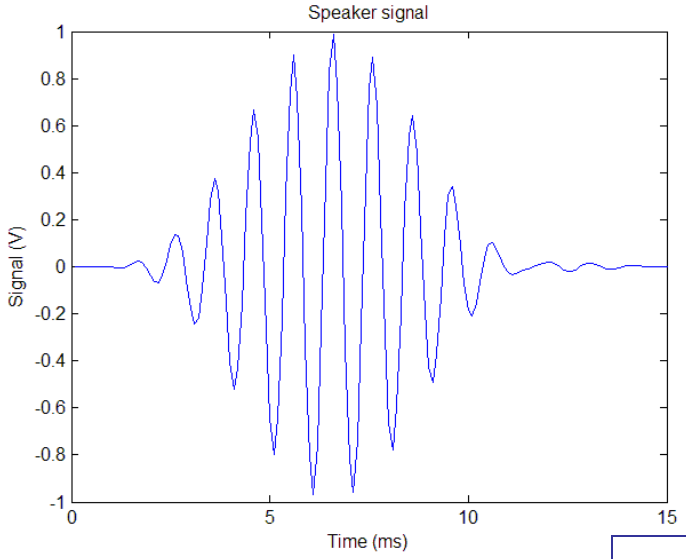

Emitted signal

Received signal

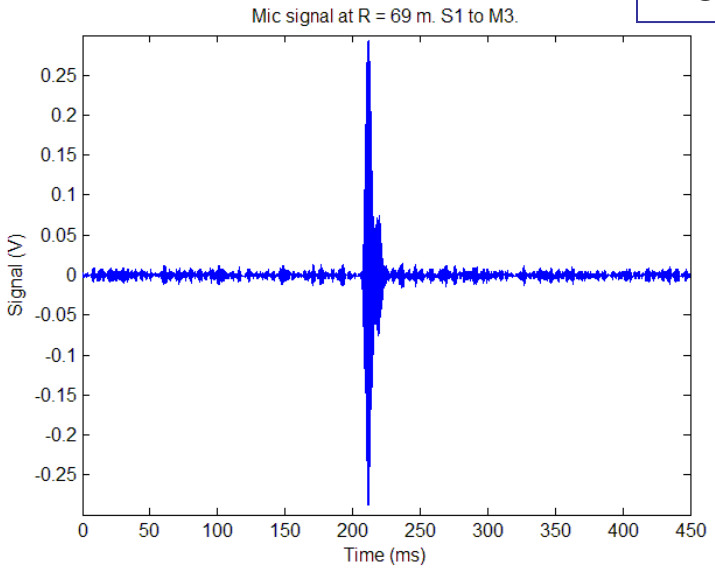

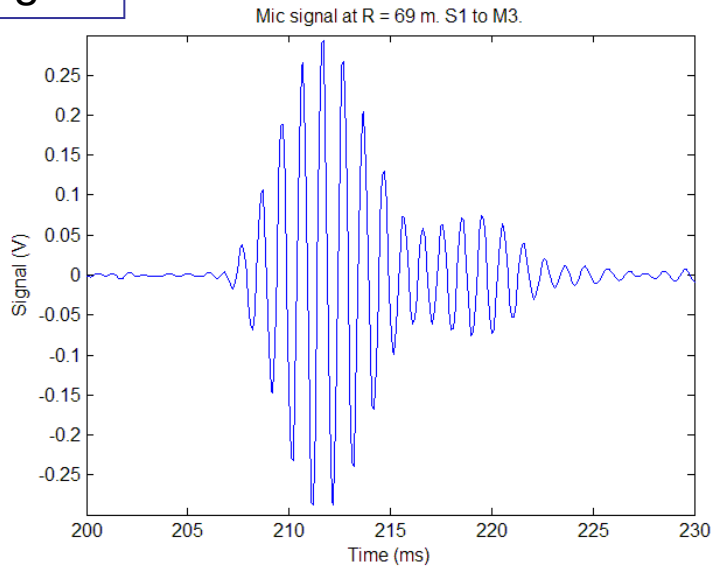

Results of ATA experiment on 3/27/2008

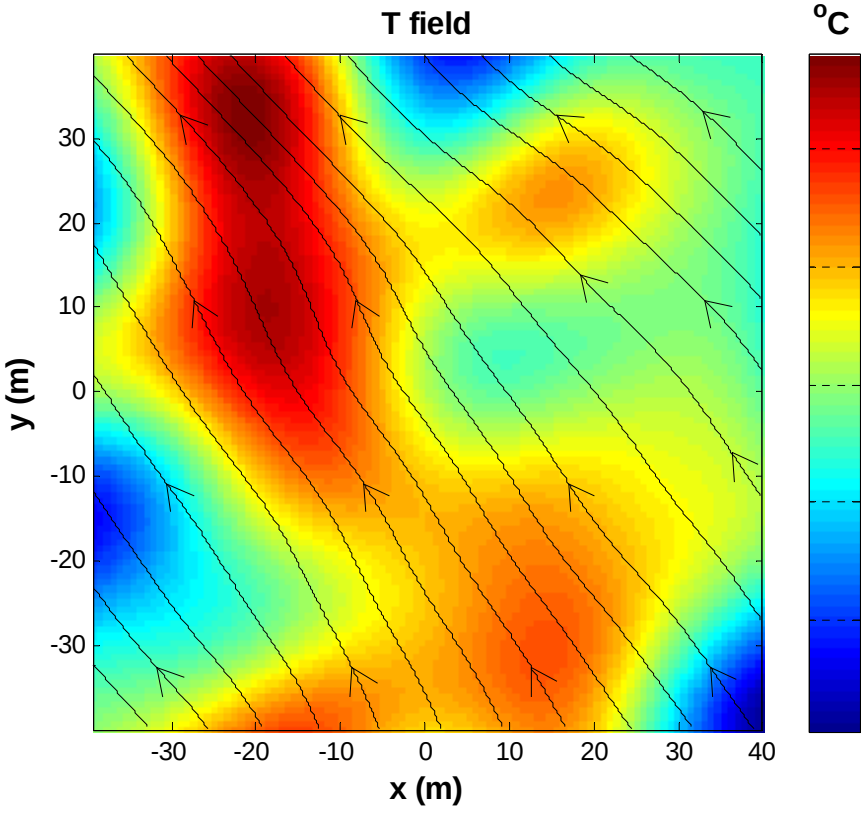

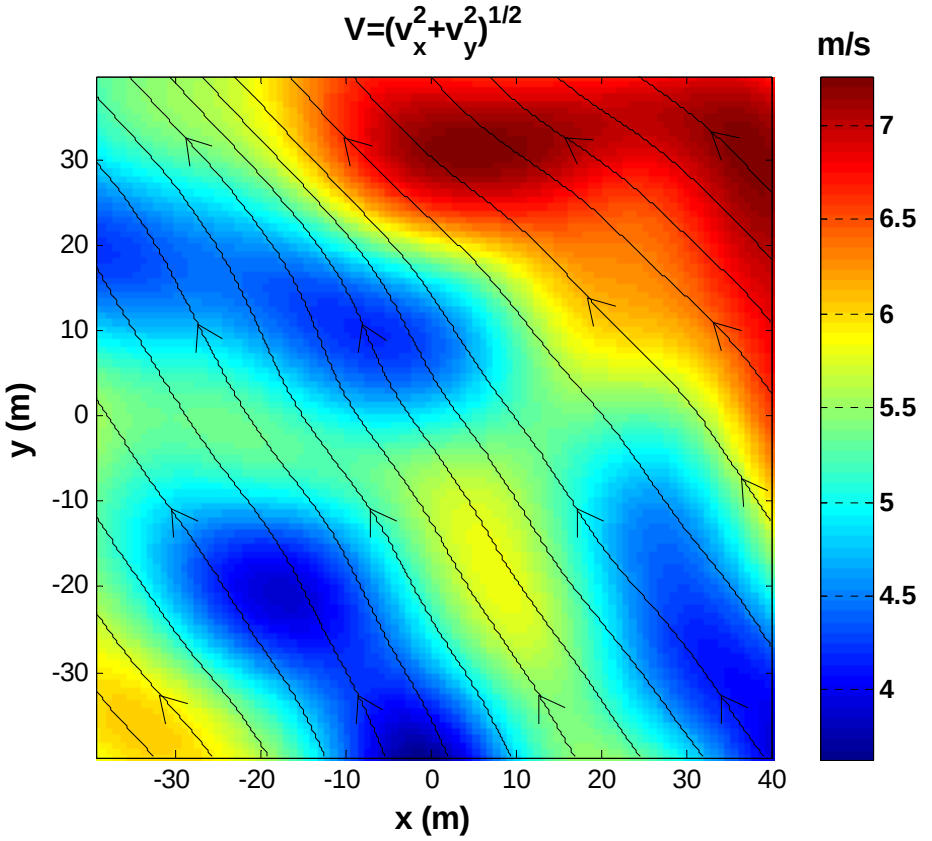

Temperature and wind velocity fields reconstructed with TDSI.
Arrows indicate the direction of the mean wind.
The values of temperature and wind velocity are realistic.
Temperature and velocity eddies are clearly seen in the plots.

Concluding Remarks

- Acoustic tomography is being used to image the dynamics of near-surface temperature and wind fields. A new array is now operational at the Boulder Atmospheric Observatory (BAO).
- One of the main issues with acoustic tomography is development of appropriate inverse algorithms. Since the problem is inherently underdetermined, some assumptions must be made.
  - The stochastic inverse method can give very good results (for point measurements as well as tomography) even when there is a mismatch between the presumed and actual correlation functions of the reconstructed field(s). It is fairly harmless to assume a correlation length that is too long.
  - Inverse methods based on grid-cell partitioning force a discontinuous solution onto a continuous field. This can lead to substantial errors.
  - Reciprocal transmissions are unnecessary, although they can be useful for resolving sound speed (temperature) when wind dominates.
- We have developed a new method called *time-dependent stochastic inversion* (TDSI) that improves reconstruction of the fields using past observations and time correlations.
- Acoustic tomography may be considered as part of a broader trend toward data assimilation and inverse reconstructions based on large quantities of disparate sensor data.